The Journal of Chemical Physics

RESEARCH ARTICLE | OCTOBER 15 1992

Laser-induced interaction of ammonia with GaAs(100). II. Desorption dynamics

X.-Y. Zhu; M. Wolf; T. Huett; J. M. White

J. Chem. Phys. 97, 5868–5875 (1992)
https://doi.org/10.1063/1.463746

AIP Publishing

Laser-induced interaction of ammonia with GaAs(100). II. Desorption dynamics

X.-Y. Zhu, M. Wolf, T. Huett, and J. M. White
Department of Chemistry and Biochemistry, Center for Materials Chemistry, University of Texas, Austin, Texas 78712

(Received 13 May 1992; accepted 6 July 1992)

UV laser irradiation of ammonia adsorbed on GaAs(100) leads to molecular desorption, with a mean translational temperature of $\langle E_{trans}/2k\rangle = 300$ K, independent of photon energy and isotope substitution. However, the photodesorption cross section depends strongly on isotope substitution: $\sigma_{NH_3}/\sigma_{ND_3}=4.1$ at $h\nu=6.4$ eV. This isotope effect is too large to be accounted for by the mass difference in the leaving particles (NH_3 vs ND_3), but can be successfully explained in terms of an isotope effect in the internal N–H(D) coordinates. We take this as evidence for uv-driven photodesorption from electronically quenched, but vibrationally hot ground state ammonia.

I. INTRODUCTION

Desorption induced by electronic transitions (DIET) is, at present, mainly explained within the qualitative framework of the Menzel–Gomer–Redhead (MGR) model[1] and its variations.[2–6] The MGR model, advanced originally to explain electron-stimulated desorption (ESD) from surfaces,[1] employs adiabatic approximations: an initial Franck–Condon transition, followed by nuclear motion on an excited potential energy surface (PES), and a second Franck–Condon transition from the nonstationary state on the excited PES back to the ground state. This second Franck–Condon transition accounts for efficient substrate-mediated relaxation (quenching) on a metal or semiconductor surface. The MGR model assumes a critical adsorbate-substrate distance, z_c, on the excited state PES. For $z>z_c$, quenching leads to desorption because the adsorbate has gained enough kinetic energy to overcome the ground state barrier leading to desorption, whereas for $z<z_c$, quenching leads to the recapture of the ground state adsorbate. It must be pointed out that quenching at $z<z_c$ may lead to vibrational excitation of the adsorbate in the ground electronic state, which is assumed to be unimportant in conventional DIET models,[1–6] but, as we will assert in this paper, is important for uv photodesorption of ammonia from GaAs(100).

The MGR model predicts an isotope effect because a lighter particle is accelerated in a shorter time on the excited PES and, thus, has a higher probability to desorb. Strong isotope effects, consistent with the MGR model, have been observed in ESD[7] and in surface photon-driven processes.[8]

Studying isotope effects has been particularly rewarding in understanding not only DIET processes, but also many other physical phenomena, e.g., dissociative electron attachment (DEA), fluorescence, superconductivity, etc. For an event of interest on an excited potential energy surface (PES), if there exists a competing decay channel, such as electron detachment in DEA or quenching by the substrate of the electronic excitation in DIET, the probability of the event depends strongly on the life time of the excited state. Classically, a heavier isotope species is accelerated more slowly on the excited PES and, thus, in competition with quenching, the probability of survival to reach the exit channel of interest is lower. This isotope effect has been frequently observed in DIET[7,8] and DEA.[9,10]

For a particle moving on a PES, starting from position z_0 to the exit channel z_e, the probability of survival, P_e, on the PES is given by

$$P_e=\exp\left[-\int_{z_0}^{z_e}\frac{R(z)dz}{v}\right], \tag{1}$$

where v is the velocity along the excited PES, and the $R(z)$ is the rate of the competing channel. Expressing v as a classical velocity, we have

$$P_e=\exp\left[-\sqrt{\frac{m}{2}}\int_{z_0}^{z_e}\frac{R(z)dz}{\sqrt{V(z_0)-V(z)}}\right], \tag{2}$$

where V is the potential energy on the excited PES and m is the reduced mass for motion on the PES. With a primary excitation cross section of σ_{ex}, assumed to be independent of isotope substitution, the effective cross section for the interested exit channel, e.g., desorption in DIET, is given by

$$\sigma_m=\sigma_{ex}P_e(m). \tag{3}$$

For two isotopic species with masses m_1 and m_2, combining Eqs. (2) and (3) gives the isotope effect

$$\frac{\sigma_{m_1}}{\sigma_{m_2}}=\left[\frac{1}{P_e(m_1)}\right]^{(m_2/m_1)^{1/2}-1}. \tag{4}$$

It is important to note that Eq. (4) is independent of the details of the PES and the competition rate, R. It is given by Newton's law of motion, provided that the excitation cross section, the potential energy surfaces, and the deexcitation rate are independent of isotope substitution. This is usually true because the electronic structure of a molecule is not significantly altered by isotope substitution.

 0021-9606/92/205868-08$006.00

In this paper, we demonstrate that the isotope effect in the uv photodesorption of ammonia from GaAs(100) is too large to be accounted for by the mass effect of the leaving particle in Eq. (4), but can be successfully explained by an isotope effect in the internal N–H coordinates. This implies uv-driven photodesorption from electronically quenched, but vibrationally hot, ground state ammonia. The proposed vibrational pumping mechanism is an alternative to the direct resonant intraadsorbate vibrational excitation by ir photon absorption that has been found in ir laser induced desorption studies.[11] A preliminary report of the work presented here has been published elsewhere.[12]

II. EXPERIMENT

All experiments were conducted in the UHV chamber described in the preceding paper[13] and involved temperature-programmed desorption (TPD), time-of-flight (TOF) mass spectroscopy, high-resolution electron-energy-loss spectroscopy (HREELS), x-ray photoelectron spectroscopy (XPS), and low-energy electron diffraction (LEED). In all experiments, ammonia was dosed through a 2μ pinhole doser onto the front face of the sample at 102 K to yield a saturation coverage of 0.5 ML. For post-irradiation TPD measurements, the full front surface of the substrate was uniformly illuminated at normal incidence. In TOF measurements, only the center portion of the sample was irradiated, with the laser light ($\phi = 5$ mm) 60° off the surface normal. The flight distance (sample to QMS ionizer) was 6 cm. The flight times were corrected for the transit time inside the QMS (11 μs for m/e = 17).

III. RESULTS

The experimental results will be presented in three sections: Section III A shows the time-of-flight distribution of ammonia as a function of laser power, photon energy, and isotope substitution; Sec. III B compares the photodesorption cross sections at 193 nm for separately adsorbed, as well as coadsorbed, NH_3 and ND_3 on GaAs(100); Sec. III C shows the wavelength dependence of photodesorption cross sections and isotope effects.

A. TIME-OF-FLIGHT DISTRIBUTIONS

As presented in the preceding paper, photon irradiation of monolayer ammonia covered GaAs(100)–(4×6) leads to molecular desorption and a small amount of photodissociation ($\leqslant 10\%$ of total photolysis). The photodesorbing ammonia is detected by the QMS in the time-of-flight (TOF) mode. Figure 1 shows four TOF spectra taken at 102 K for 0.5 ML NH_3–GaAs(100) at 193 nm. All spectra were averaged over 128 laser shots with the indicated pulse energies (from top to bottom: 10.5, 7.8, 2.8, 0.8 mJ /cm^2). While the shape of all spectra are identical, the intensity increases linearly with laser pulse energy (see below). Each spectrum yields a mean translational energy of $\langle E_{trans}/2k\rangle = 300 \pm 30$ K, independent of laser pulse energy, indicating a nonthermal desorption mechanism. Strong support for the nonthermal mechanism is also given

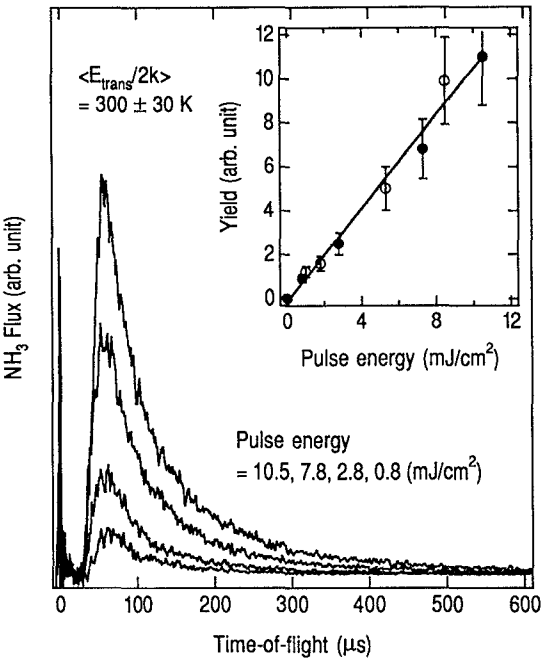

FIG. 1. NH_3 time-of-flight (TOF) spectra from 0.5 ML NH_3–GaAs(100) at 102 K and 193 nm. Each spectrum was averaged over 128 laser shots with the indicated laser pulse energy (from top to bottom, 10.5, 7.8, 2.8, and 0.8 mJ/cm^2). The flux-weighted average translational energy for photodesorbing NH_3, derived from numerical integration of the data, is $\langle E_{trans}/2k\rangle = 300 \pm 30$ K, independent of pulse energy. Inset: Laser pulse energy dependence of NH_3 photodesorption yield. Solid circles are integrated fluxes of the TOF spectra and open circles are from post-irradiation NH_3 TPD areas, $\ln(I_0/I)$. Solid line is a least-square linear fit to the data.

by the laser pulse energy dependence of photodesorption yield in the inset, obtained from both TOF (solid circles) and TPD (open circles) measurements. Within experimental error, the yield is linear with pulse energy, clearly establishing a nonthermal excitation mechanism.

Changing the laser wavelength, Fig. 2 compares the NH_3 TOF distributions from 0.5 ML NH_3–GaAs(100) at 193 and 248 nm. While the intensity of the TOF distribution at 248 nm is $\frac{1}{5}$ of that at 193 nm, both spectra give mean translational temperatures of 300 ± 30 K. This result points to a common desorption mechanism at both wavelengths. Similar results are obtained for 351 nm.

The TOF distribution of photodesorbing ammonia is also independent of isotope substitution (Fig. 3). The inset compares the translational energy distributions of NH_3 (solid) and ND_3 (dashed, ×4) obtained from the TOF spectra in Fig. 4 at 193 nm. Clearly, within experimental uncertainty, the translational energy distributions for NH_3 and ND_3 are identical, both giving a mean translational energy of 52 ± 5 meV, or $\langle E_{trans}/2k\rangle = 300 \pm 30$ K. Also shown in the inset (dotted curve) is a Maxwell–Boltzmann distribution with a mean translational energy of 52 meV, or $\langle E_{trans}/2k\rangle = 300$ K. Interestingly, both translational distributions deviate from the Maxwell–Boltzmann distribution.

As shown in Fig. 3, while the TOF distribution of

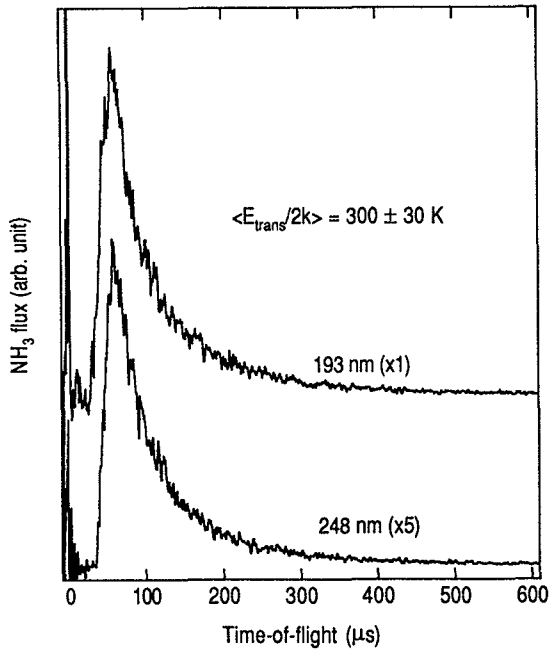

FIG. 2. NH_3 TOF spectra from 0.5 ML NH_3–GaAs(100) at 193 (upper) and 248 nm (lower, ×5). Each spectrum was averaged over 1×10^{18} photons/cm^2. A laser pulse energy of 1 mJ/cm^2 was used for measurements at both wavelengths. The flux-weighted average translational energy for photodesorbing NH_3 is $\langle E_{trans}/2k\rangle = 300\pm30$ K, independent of wavelength. The presented spectrum at 248 nm is multiplied by a factor of 5.

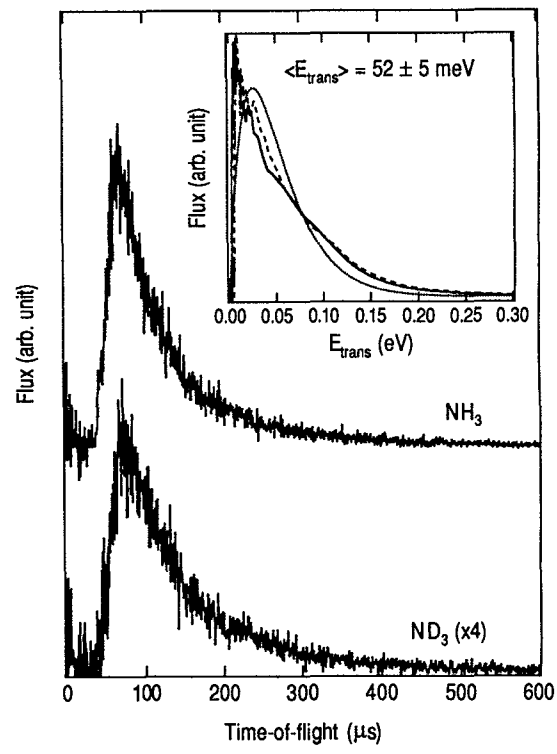

FIG. 3. TOF spectra of NH_3 (upper) and ND_3 (lower, ×4) taken at 193 nm for 0.5 ML NH_3 and 0.5 ML ND_3 covered GaAs(100) surfaces, respectively. Each spectrum was averaged over 1×10^{18} photons/cm^2. A laser pulse energy of 1 mJ/cm^2 was used for both measurements. The inset shows the smoothed spectra in the energy domain (solid and dashed spectra for NH_3 and ND_3, respectively). The flux-weighted average translational energy is $\langle E_{trans}/2k\rangle = 52\pm5$ meV or 300 ± 30 K, independent of isotope substitution. Also shown in the inset is a Maxwell–Boltzmann distribution (dotted curve) with a mean energy of 52 meV. The ND_3 spectra are presented with a multiplication factor of 4.

photodesorbing ammonia is, within experimental uncertainty, independent of isotope substitution, the *intensity* of photodesorbing NH_3 is more than four times that for ND_3, indicating a very strong isotope effect in the photodesorption cross section. In the following, we turn to a quantitative assessment of this isotope effect using post-irradiation temperature-programmed desorption.

B. Isotope effect at 193 nm

Figure 4 shows the molecular ammonia coverage, obtained from post irradiation TPD areas, as a function of photon fluence at $h\nu=6.4$ eV for both NH_3 and ND_3 covered surfaces. The photodissociation channel makes a negligible contribution;[13] thus, the slopes measure the photodesorption cross sections. Least-square fits to the data yield, for ammonia photodesorption from GaAs(100) at 6.4 eV, $\sigma_{NH_3}=5.4\times10^{-20}$ cm^2, and $\sigma_{ND_3}=1.3\times10^{-20}$ cm^2. Therefore, the isotope effect is $\sigma_{NH_3}-\sigma_{ND_3}=4.1\pm0.5$, in agreement with the TOF results presented in Fig. 3.

In order to understand whether the desorption process is localized, we have also measured the isotope effect in coadsorbed isotopic mixtures of ammonia on GaAs(100). In this experiment, equal amounts of NH_3 and ND_3 were mixed at room temperature in a stainless steel gas reservoir. Mass analysis showed complete isotope mixing, giving a $[NH_3]$:$[NDH_2]$:$[NHD_2]$:$[ND_3]$ ratio of 2:5:5:2 (±10%). This mixture was dosed onto the GaAs(100)-(4×6) surface at 102 K. In TPD, all masses between m/e=14 and 20 were followed. A deconvolution procedure using calibrated ammonia QMS cracking patterns was employed to obtain the coverage of each isotope labeled ammonia. Figure 5 plots, on a semilogarithmic scale, the normalized coverages of all labeled ammonia molecules as a function of photon fluence at $h\nu=6.4$ eV. With no irradiation, the starting coverages are 0.07, 0.18, 0.18, and 0.07 ML for NH_3, NDH_2, NHD_2, and ND_3, respectively. As shown in the upper panel, NH_3 is depleted much faster than ND_3 by photon irradiation. An isotope effect of $\sigma_{NH_3}/\sigma_{ND_3}=3.6\pm0.7$ is obtained for the photodesorption cross section from coadsorbed NH_3 and ND_3. Within experimental uncertainty, this isotope effect is the same as that in Fig. 4. The photodesorption cross sections of NDH_2 and NHD_2 lie between the values for NH_3 and ND_3.

C. Wavelength dependences

The isotope effect in ammonia photodesorption was also measured at photon energies of 5.0 and 3.5 eV. Figure 6 shows, in semilogarithmic form, the ammonia coverages for both NH_3 and ND_3 saturated GaAs(100) surfaces as a function of photon exposure at $h\nu=5.0$ eV (lower panel) and 3.5 eV (upper panel). Least-square fits to the data yield photodesorption cross sections: at $h\nu=5.0$ eV, σ_{NH_3}

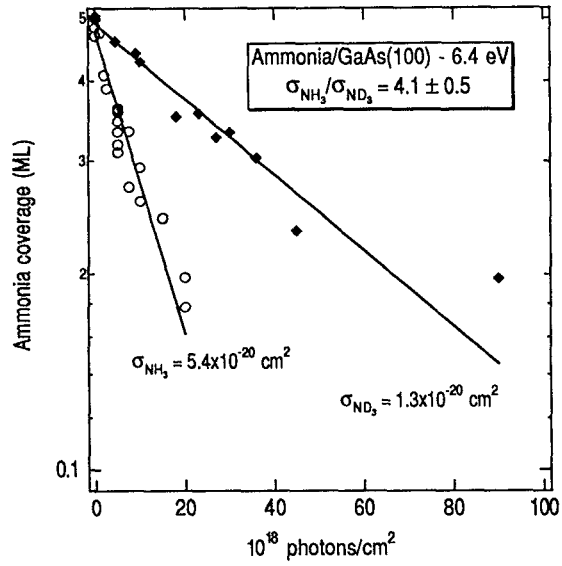

FIG. 4. Post-irradiation TPD areas for NH_3 (open circles) and ND_3 (solid diamonds) as a function of photon fluence at 6.4 eV (193 nm) for both NH_3 and ND_3 covered (0.5 ML) GaAs(100). Least-square linear fits to the data result in photodesorption cross sections of 5.4×10^{-20} and 1.3×10^{-20} cm^2 for NH_3 and ND_3, respectively. This gives an isotope effect, $\sigma_{NH_3}/\sigma_{ND_3}$, of 4.1 ± 0.5.

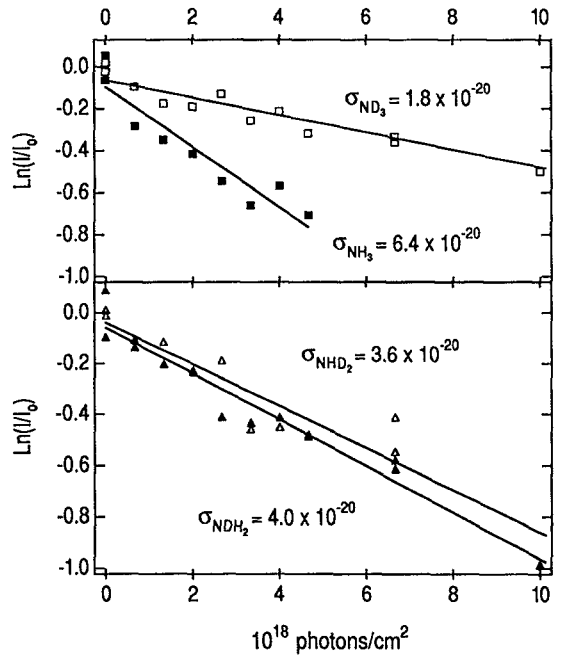

FIG. 5. Post-irradiation TPD areas for NH_3 (solid squares), ND_3 (open squares), NDH_2 (solid triangles), and NHD_2 (open triangles) as a function of photon fluence at 6.4 eV from a GaAs(100) surface saturated with isotopic mixed ammonia at 102 K (0.07 ML NH_3, 0.07 ML ND_3, 0.18 ML NHD_2, and 0.18 ML NDH_2). All data points are normalized to those with no irradiation and presented in a semilogarithmic form. Least-square linear fits to the data result in photodesorption cross sections of 6.4×10^{-20}, 4.0×10^{-20}, 3.6×10^{-20}, and 1.8×10^{-20} cm^2 for NH_3, NDH_2, NHD_2, and ND_3, respectively.

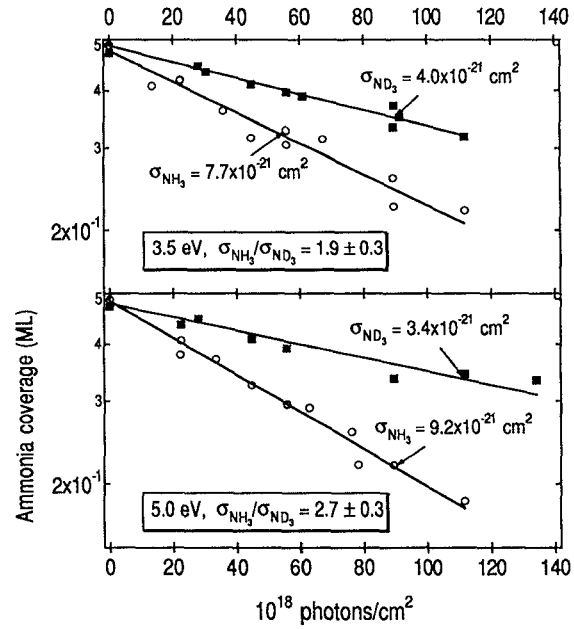

FIG. 6. Post-irradiation TPD areas for NH_3 (open circles) and ND_3 (solid squares) as a function of photon fluence at $h\nu=5.0$ eV (lower panel) and 3.5 eV (upper panel) for both NH_3 and ND_3 covered (0.5 ML) GaAs(100). Least-square linear fits (solid lines) to the data give photodesorption cross sections indicated on the figure. This gives isotope effects, $\sigma_{NH_3}/\sigma_{ND_3}$, of 2.7 ± 0.3 and 1.9 ± 0.3 for $h\nu=5.0$ and 3.5 eV, respectively.

$=9.2\times10^{-21}$ cm^2, and $\sigma_{ND_3}=3.4\times10^{-21}$ cm^2; at $h\nu=3.5$ eV, $\sigma_{NH_3}=7.7\times10^{-21}$ cm^2, and $\sigma_{ND_3}=4.0\times10^{-21}$ cm^2. This gives $\sigma_{NH_3}/\sigma_{ND_3}=2.7\pm0.3$ and 1.9 ± 0.3 at $h\nu=5.0$ and 3.5 eV, respectively. The obtained cross sections and isotope effects are summarized in Table I.

Figure 7 shows the photon energy dependence of photodesorption cross sections (open circles for NH_3 and solid triangles for ND_3. Also shown is the GaAs absorbance (dashed line, right axis)[14] and, as described below, the calculated initial excitation cross sections, σ_{ex} (crosses).

IV. DISCUSSION

As we will demonstrate in the following, photodesorption of ammonia on GaAs results from electronically quenched, but vibrationally hot, ground state adsorbates. In this mechanism, excitation and deexcitation of the electronic state of adsorbed ammonia leads to internally excited ammonia. The vibrational energy in the internal modes can couple to the ammonia-substrate bond and lead to molecular desorption. We separate the process into three steps: (i) the initial electronic excitation followed by (ii) propagation of the system on the excited potential energy surface and quenching of the excited state to yield vibrationally excited ammonia, and (iii) transfer of the vibrational energy in the internal modes of ammonia to the surface-NH_3 coordinate, leading to molecular desorption. Step (i) is assumed to follow the Franck–Condon approximation. Steps (ii) and (iii) are, to the first approximation, separable because the lifetimes of electronically and vibra-

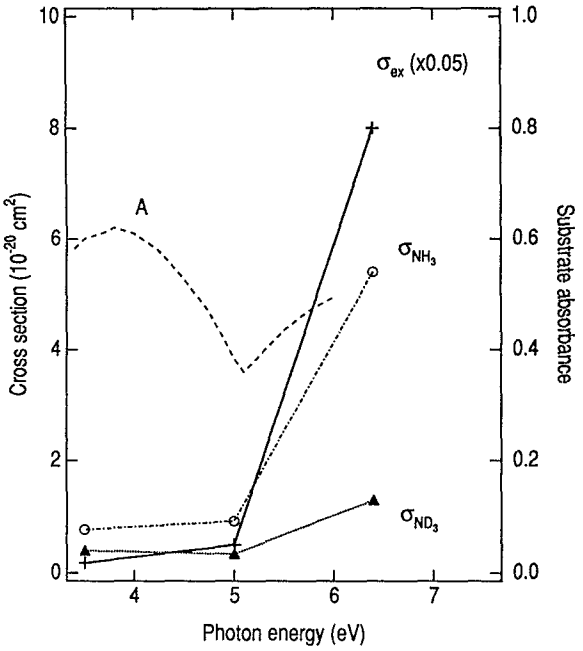

FIG. 7. Photon energy dependence of photodesorption cross sections: open circles (dot-dashed line) for σ_{NH_3}, solid triangles (dotted line) for σ_{ND_3}, and solid crosses (solid line) for the calculated excitation cross section. The dashed curve is the substrate absorbance (A = 1-reflectivity), reproduced from Ref. 14.

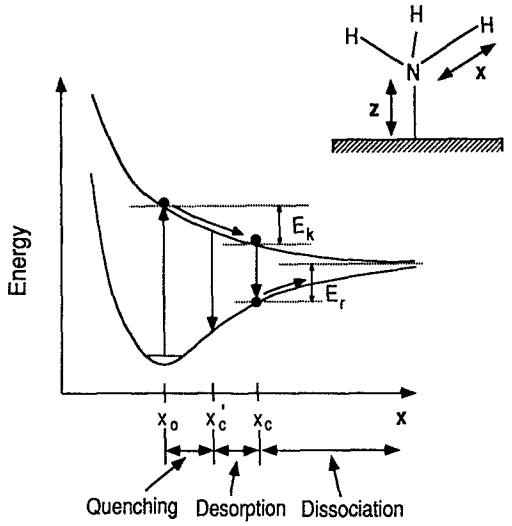

FIG. 8. Schematic energy diagram of the proposed model for photodesorption from electronically quenched adsorbate. The x corresponds to the N–H distance in NH_3 and the z corresponds to the surface-NH_3 distance. Photon-driven excitation moves the system to the excited PES, assumed to be repulsive with respect to the N–H bond, but can be of any shape. If deexcitation occurs at $x > x_c$, the H atom has gained enough kinetic energy to overcome the recapture barrier and lead to dissociation, with a escape probability of P_e. For $x_c' < x < x_c$, the N–H vibrational energy in the "recaptured" NH_3 is sufficient to overcome the thermal desorption barrier, provided it transfers to the z.

tionally excited states are on the order of 10^{-15} (Refs. 1–6) and 10^{-11} (Refs. 11 and 15) s, respectively. We discuss each step as follows.

A. Excitation

The linear power dependence and the independence of translational energy on laser power in Fig. 1 clearly establish a nonthermal excitation mechanism. We now discuss the two possible electronic excitations which may lead to the observed photochemistry: (i) direct photon absorption by adsorbed ammonia and (ii) substrate mediated excitation, including the attachment of photoexcited substrate carriers and photoassisted charge transfer from surface states to the adsorbate. The direct excitation mechanism cannot play a role at $h\nu = 3.5$ eV, which is 2 eV below the gas phase absorption threshold.[16] As discussed in the preceding paper,[13] it is unlikely that the uv absorption threshold of ammonia can be red shifted by more than 2 eV through adsorption while its vibrational frequencies are only slightly perturbed. Therefore, we conclude that the photoexcitation is exclusively substrate mediated at $h\nu = 3.5$ eV, probably involving the attachment of photoexcited substrate electrons. This leads to an important question: Is this mechanism dominant at all photon energies? To answer this question, we now examine the wavelength dependence in Fig. 7.

As shown in Fig. 7, the photodesorption cross sections of both NH_3 and ND_3 remain nearly constant at $h\nu = 3.5$–5.0 eV, but increases significantly when the photon energy is increased to 6.4 eV, implying a possible change in excitation mechanism. A similar trend is seen for the excitation cross section (see below). This behavior does not correlate with changes in the substrate absorbance (A, dashed curve in Fig. 7), which varies no more than $\pm 30\%$ between 3 and 6 eV.[14] In view of the gas phase photochemistry of ammonia,[16] we suggest that, at $h\nu > 5.0$ eV, in addition to the substrate mediated process, a direct excitation mechanism is operative. This interpretation can successfully explain the wavelength dependences in Fig. 7. The similar wavelength responses for both photodissociation and photodesorption, as discussed in the preceding paper,[13] suggest the same excitation for both photolysis channels.

B. Desorption from electronically quenched adsorbate

Having discussed the excitation mechanism, we now turn to the mechanism for photodesorption. We first demonstrate the inability of DIET models, which assumed the mass of the desorbing fragment is critical, to describe ammonia photodesorption from GaAs(100). Using Eq. (4) with a mass ratio of $m_{NH_3}/m_{ND_3} = 1.176$ and the measured isotope effect at 6.4 eV, $\sigma_{NH_3}/\sigma_{ND_3} = 4.1 \pm 0.5$, we obtain an escape probability of $P_e(NH_3) = 5.5 \times 10^{-8}$. This results in a photoexcitation cross section, $\sigma_{ex} = \sigma_{NH_3}/P_e$, of $\sim 1 \times 10^{-12}$ cm^2 or 10000 Å^2, which is unrealistically large. We now examine how the internal N–H excitation, i.e., vibrational excitation which can realistically have a much larger isotope effect, might lead to desorption.

The proposed mechanism, shown schematically in Fig. 8, is a variation of the MGR model. We assume the initial

TABLE I. Photodesorption cross sections (cm^2).

		193 nm	248 nm	351 nm
NH_3	σ_{des}	5.4×10^{-20}	9.2×10^{-21}	7.7×10^{-21}
ND_3	σ_{des}	1.3×10^{-20}	3.4×10^{-21}	4.0×10^{-21}
Isotope effect ($\sigma_{NH_3}/\sigma_{ND_3}$)		4.1 ± 0.5	2.7 ± 0.3	1.9 ± 0.2
Excitation, σ_{ex} (calculated)		1.6×10^{-18}	1.0×10^{-19}	3.6×10^{-20}

Franck–Condon transition involves uv photon excitation, either directly or through the substrate, to give an electronically excited molecule. This excited state is antibonding, with respect to N–H, as is the case for gas-phase photodissociation and dissociative electron attachment.[10,16] While a small fraction of the excited state may lead to dissociation, as observed experimentally, most of the excited ammonia is quenched to give vibrationally excited NH_3 on the ground state PES. This scenario is so far consistent with conventional MGR models. However, unlike the conventional MGR model, which takes no account of the vibrationally excited adsorbate on the ground state PES, we suggest that the vibrational energy in the N–H coordinate (x) is coupled to the N-surface coordinate (z) and, if sufficient energy transfers, desorption follows. The common excited state for both desorption and dissociation accounts for the observation of similar wavelength dependences for both photolysis channels, as presented in the preceding paper.[13] The vibrational energy transfer process has already been demonstrated in ir laser induced desorption of NH_3 from metal and dielectric surfaces, where resonant excitation of the ν_s stretching mode of adsorbed NH_3 leads to molecular desorption.[11(e)] We will go into more detail on this vibrational energy transfer process in the next section.

We introduce two critical distances in the stretch of N–H, x_c and x_c'. For deexcitation occurring at $x > x_c$, the kinetic energy, E_k, (in this case of the H atom) is greater than the barrier for dissociation, E_r, and the coordinate x is not bound (dissociation). The reverse holds for $x < x_c$. We assume a *second* critical distance, x_c': deexcitation at $x > x_c'$ results in a ground state NH_3 adsorbate with sufficient *intramolecular* vibrational content to undergo the aforementioned vibrational energy transfer, and desorb. The probability of desorption, P_d, is equal to the fractional population that is formed by quenching within the range, $x_c' < x < x_c$,

$$P_d = P_e(x_c') - P_e(x_c), \tag{5}$$

where P_e is given by Eq. (2). Since the dissociation probability, $P_e(x_c)$, is only $\leqslant 10\%$ of the desorption probability, P_d, the second term in Eq. (5) can be neglected and the desorption probability (P_d) is given by $P_e(x_c')$. Therefore, a modified form of Eq. (4) can be derived to give the isotope effect

$$\frac{\sigma_{NH_3}}{\sigma_{ND_3}} = \left[\frac{1}{P_d(NH_3)}\right]^{(m_D/m_H)^{1/2}-1}, \tag{6}$$

where m_D and m_H are the *masses of the H and D atoms*, which approximate the reduced masses in the N–H(D) coordinate.

It is important to note that, in addition to the stretching mode, the inversion mode of adsorbed ammonia may play an equally important role in the desorption process. It is well known that, while pyramidal in the electronic ground state, ammonia has a planar D_{3h} symmetry in the first excited state for both direct photon absorption and electron attachment.[10,16] Therefore, similar to Fig. 8, excitation and deexcitation of the electronic state of adsorbed ammonia will also lead to vibrational excitation in the inversion mode. If we assume a critical bending angle, above which deexcitation results in sufficient vibrational content in the bending mode to undergo the energy transfer and desorb, the isotope effect in molecular desorption is also given by Eq. (6). The masses of the H and D atoms approximate the reduced masses in the N–H(D) bending coordinate.

Equation (6) differs from Eq. (4) in that the masses in the former are not those for the leaving particle, but the reduced masses in the N–H and N–D coordinate where the energy for photodesorption is fed in. From the measured isotope effect of $\sigma_{NH_3}/\sigma_{ND_3} = 4.1$ at $h\nu = 6.4$ eV, and the mass ratio of $m_D/m_H = 2$, we obtained a photodesorption probability of $P_d = 0.033$ for NH_3. Similarly, at $h\nu = 5.0$ and 3.5 eV, the calculated photodesorption probabilities are $P_d = 0.091$ and 0.21, respectively. The excitation cross sections follow $\sigma_{ex} = \sigma_{NH_3}/P_d = 1.6 \times 10^{-18}$, 1.0×10^{-19}, and 3.6×10^{-20} cm^2 at $h\nu = 6.4$, 5.0, and 3.5 eV, respectively. These values are listed in Table I and Fig. 7, and are all intuitively reasonable.

It is interesting that the isotope effect depends on photon energy (Table I). Since the probability of desorption depends on the details of the potential energy surfaces and the quenching rate [Eq. (2)], it should depend strongly on the excitation mechanism (direct photon absorption vs substrate-mediated electron transfer). As discussed above, substrate mediated excitation dominates at $h\nu = 3.5$ eV, while direct photon absorption may contribute significantly at $h\nu = 6.4$ eV. At 5.0 eV, a slight red shift in ammonia uv absorption upon adsorption on the GaAs(100) surface can result in a situation where both direct and substrate-mediated excitations are important. This is a plausible explanation for the wavelength dependence of these isotope effects.

In the following, we discuss possible mechanisms for the last step: desorption from vibrationally excited NH_3 on GaAs(100).

C. The vibrational energy transfer process

Desorption stimulated by excitation of an internal vibration of an adsorbed molecule has been the subject of intense experimental and theoretical investigations.[11] In these studies, an internal vibrational mode in an adsorbed molecule is resonantly pumped via the absorption of single or multiple ir photons. Subsequent relaxation of the vibrationally excited adsorbate, with energy above the desorption continuum, can lead to molecular desorption via three possible mechanisms:[11] (i) A resonant heating process occurs in which the adsorbate-surface coupling leads to the excitation of substrate phonons. If the adsorbate-surface vibration absorbs one phonon, the instantaneous vibrational energy in this bond can exceed the binding energy and desorption follows. (ii) A resonant tunneling process occurs where the internal vibrationally excited state is resonant with a desorption continuum state. Tunneling into the latter state results in desorption. (iii) A phonon-assisted inelastic tunneling process occurs in which tunneling is aided by the emission or absorption of phonons.

All three mechanisms can contribute to ir laser induced desorption. In ir laser induced desorption of ammonia and pyridine from metal and dielectric surfaces, Chuang and co-workers found the resonant heating mechanism to be most important.[11(c),(e)] This conclusion was drawn from the observation that resonant excitation of one isotopically-labeled species for coadsorbed NH_3 and ND_3 led to the desorption of both. If a similar mechanism were operative for ammonia desorption from GaAs(100), we would expect that the isotope effect in desorption cross sections should be removed upon coadsorption of NH_3 and ND_3. However, the results in Fig. 5 clearly show that the large isotope effect in desorption cross sections is still present for coadsorbed NH_3 and ND_3 on GaAs(100). Therefore, the resonant heating mechanism is not favored here, at least with the adsorbate coverages used ($\leqslant 0.5$ ML). We suggest that the vibrationally excited ground state ammonia on GaAs(100) undergoes the localized tunneling-relaxation process for desorption [mechanisms (ii) and (iii) mentioned above]. The reduced mass in the internal coordinate increases in the order of NH_3, NDH_2, NHD_2, and ND_3, thus, the cross section of vibration-mediated desorption decreases in the same order, as shown in Fig. 5.

We now estimate the energetics of this vibrational energy transfer process. As presented in the preceding paper, the binding energy (D_0) of molecular NH_3 on GaAs(100)-(4×6) is 0.35 eV at 0.5 ML, and the surface-NH_3 stretching frequency is $\omega_0=820$ cm^{-1}.[13] Figure 9 shows a model Morse potential representing the surface-adsorbate, S–NH_3, interaction

$$V_{\text{S-NH}_3}=D_0(1-e^{-\beta z})^2, \tag{7}$$

where we have taken $D_0=0.4$ eV; $\beta=0.5\omega_0(2\mu/D_0)^{1/2}$ and μ, the reduced mass, is equal to m_{NH_3}, 17 amu. This potential will support seven vibrational states. Also shown in Fig. 9 is a harmonic potential ($\omega'=3340$ cm^{-1}) for the N–H coordinate (dashed curve, different coordinate).

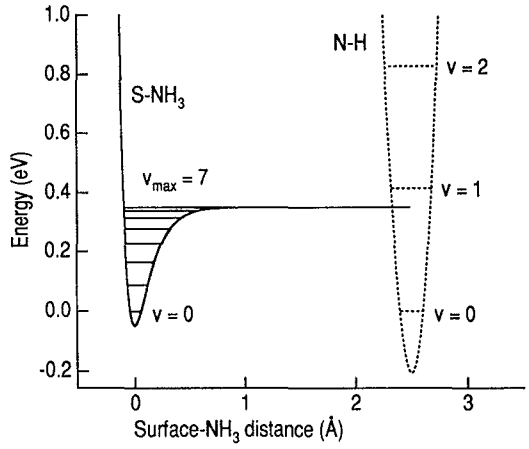

FIG. 9. Potential energy surface (solid curve) for the GaAs–NH_3 potential, which is taken to be a Morse potential as described in the text. Solid lines are the vibrational energy levels of the Morse potential. The ground ($v=0$) vibrational energy level is used as the reference for the y-axis. The x-axis represents the surface-NH_3 distance, with the equilibrium position as the reference. Dashed curve shows a harmonic potential (in a different coordinate) for the N–H internal stretching mode.

Clearly, an internally excited NH_3 with $v\geqslant 1$ can be degenerate with some continuum state of momentum p, rotational excitation J and internal excitation $v'(\leqslant v-1)$ as follows:

$$\left(v+\frac{1}{2}\right)\hbar\omega'=\frac{p^2}{2m}+\left(v'+\frac{1}{2}\right)\hbar\omega'+J(J+1)\hbar\Omega_r. \tag{8}$$

Not included in Eq. (8) are the inversion-vibrational mode, as discussed in Sec. IV B, and the surface phonon modes ($\pm\hbar\omega_p$), which may play equally important roles. Coupling of the internal (N–H) and external (S–NH_3) vibrations can lead to tunneling, as described by Eq. (8).

The non-Maxwell–Boltzmann (MB) translational energy distribution in Fig. 3 is consistent with the tunneling mechanism in the sense that an E_{trans} distribution broader than the MB distribution is expected.[11(b),(f)] Temperature programmed desorption spectra show negligible differences between NH_3 and ND_3, indicating that, if they exist, the thermal desorption barriers are the same for both isotopes. This is sensible because isotope substitution has little effect on the surface-N bond. Thus, as expected, the translational energy distributions for NH_3 and ND_3 are similar (Fig. 3). It is also worth noting that, since desorption is attributed to vibrationally excited ground state ammonia, independent of the initial electronic excitation mechanism (direct vs substrate mediated), the ammonia translational energy distribution should be relatively independent of uv photon energy, as is the case in Fig. 2.

While the above interpretation successfully explains the large isotope effect observed in ammonia photodesorption from GaAs(100), many interesting questions remain unanswered. For example, how important is the inversion vibrational mode of ammonia in the desorption process? What is the isotope effect in each of the three steps: excitation, deexcitation, and vibrational energy transfer? For

example, in some DEA systems, small inverse isotope effects have been observed.[9,10] The ground state wave function of a heavier isotopic molecule is more spatially restricted (deeper in the potential well), and thus, has a higher amplitude at the peak than the lighter molecule. This leads to a small inverse isotope effect for the excitation cross section at the peak of the resonance.[9,10] A similar inverse isotope effect in σ_{ex} [Eq. (3)], if present, will not alter our interpretation, but will affect the quantitative outcome. Unfortunately, within a classical picture, we do not know whether there is a small inverse or direct isotope effect in the deexcitation step. A semiclassical wavepacket dynamics study, currently underway,[17] may help answer these questions.

V. CONCLUSIONS

To summarize, nonthermal uv photodesorption of ammonia from GaAs(100) is characterized by a mean translational temperature of $\langle E_{trans}/2k\rangle = 300$ K, independent of photon energy ($h\nu = 6.4$, 5.0, and 3.5 eV) and isotope substitution. The photodesorption cross section depends strongly on isotope substitution. The measured isotope effect is too large to be accounted for by the mass difference in the leaving particles (NH_3 vs ND_3), but can be successfully explained by an isotope effect in the internal N–H(D) coordinates. The role of electronically quenched but vibrationally "hot" ground state adsorbate is demonstrated for the first time for DIET.

ACKNOWLEDGMENT

We thank E. Hasselbrink for delightful discussions. This work was supported in part by the Science and Technology Center Program of the National Science Foundation, Grant No. CHE-8920120.

[1] (a) D. Menzel and R. Gomer, J. Chem. Phys. **41**, 3311 (1964); (b) P. A. Redhead, Can. J. Phys. **42**, 886 (1964).
[2] P. R. Antoniewicz, Phys. Rev. B **21**, 3811 (1980).
[3] Ph. Avouris and R. E. Walkup, Ann. Rev. Phys. Chem. **40**, 173 (1989).
[4] R. D. Ramsier and J. T. Yates, Jr., Surf. Sci. Rep. **12**, 243 (1991).
[5] X.-L. Zhou, X.-Y. Zhu, and J. M. White, Surf. Sci. Rep. **13**, 73 (1991).
[6] (a) J. W. Gadzuk, Ann. Rev. Phys. Chem. **39**, 395 (1988); (b) J. W. Gadzuk, L. J. Richter, S. A. Buntin, D. S. King, and R. R. Cavanagh, Surf. Sci. **235**, 317 (1990); (c) J. W. Gadzuk, Phys. Rev. B **44**, 13466 (1991).
[7] (a) T. E. Madey, J. T. Yates, Jr., D. A. King, and C. J. Uhlander, J. Chem. Phys. **52**, 5215 (1970); (b) W. Jelend and D. Menzel, Chem. Phys. Lett. **21**, 178 (1973); (c) C. Klauber, M. D. Alvey, and J. T. Yates, Jr., Surf. Sci. **154**, 139 (1985).
[8] (a) M. Wolf, S. Nettesheim, J. M. White, E. Hasselbrink, and G. Ertl, J. Chem. Phys. **94**, 4609 (1991); (b) S. K. Jo, J. Kiss, M. E. Castro, and J. M. White, Proc. Ann. Sym. ACS (in press); (c) X.-Y. Zhu, M. Wolf, and J. M. White, J. Chem. Phys. (in press).
[9] *Electron-Molecule Interactions and Their Applications*, edited by L. G. Christophorou (Academic, New York, 1984).
[10] (a) T. E. Sharp and J. T. Dowell, J. Chem. Phys. **50**, 3024 (1969); (b) K. L. Strocklett and P. D. Burrow, J. Phys. B **19**, 4241 (1986).
[11] (a) Z. W. Gortel, H. J. Piercy, and R. Teshima, Phys. Rev. B **27**, 5066 (1983); (b) Z. W. Gortel, H. J. Piercy, and R. Teshima, Phys. Rev. B **29**, 6926 (1983); (c) T. J. Chuang, Surf. Sci. Rep. **3**, 1 (1983); (d) T. F. George, J. Lin, A. C. Beri, and W. C. Murphy, Prog. Surf. Sci. **16**, 139 (1984); (e) T. J. Chuang, H. Seki, and I. Hussla, Surf. Sci. **158**, 525 (1985); (f) J. Heidberg, H. Stein, E. Riehl, Z. Szilagyi, and H. Weiss, Surf. Sci. **158**, 553 (1985).
[12] X.-Y. Zhu and J. M. White, Phys. Rev. Lett. **68**, 3359 (1992).
[13] X.-Y. Zhu, M. Wolf, T. Huett, and J. M. White, J. Chem. Phys. **97**, 5856 (1992).
[14] K. Jezierski, Z. Gumienny, and J. Misiewicz, Appl. Surf. Sci. **50**, 341 (1991).
[15] E. J. Heilweil, M. P. Casassa, R. R. Cavanagh, and J. C. Stephenson, Ann. Rev. Phys. Chem. **40**, 143 (1989).
[16] M. N. R. Ashfold, C. L. Bennett, and R. N. Dixon, Chem. Phys. **93**, 293 (1985).
[17] X.-Y. Zhu and J. M. White (to be published).